Hindawi Publishing Corporation
International Journal of Photoenergy
Volume 2016, Article ID 2782607, 10 pages
http://dx.doi.org/10.1155/2016/2782607

Research Article

Enhanced Photocatalytic Degradation and Mineralization of Furfural Using UVC/TiO_2/GAC Composite in Aqueous Solution

Bahram Ghasemi,[1] Bagher Anvaripour,[1] Sahand Jorfi,[2,3] and Neematollah Jaafarzadeh[2,3]

[1]*Abadan Faculty of Petroleum Engineering, Petroleum University of Technology, Abadan, Iran*
[2]*Environmental Technologies Research Center, Ahvaz Jundishapur University of Medical Sciences, Ahvaz, Iran*
[3]*Department of Environmental Health Engineering, School of Health, Ahvaz Jundishapur University of Medical Sciences, Ahvaz, Iran*

Correspondence should be addressed to Bagher Anvaripour; anvaripour@put.ac.ir

Received 16 August 2016; Revised 2 November 2016; Accepted 6 December 2016

Academic Editor: Alberto Alvarez

Titanium dioxide nanoparticles were immobilized on granular activated carbon (GAC) as a porous and low-density support for photocatalytic degradation of furfural. The TiO_2/GAC composite was synthetized using the simple sol-gel method and fully characterized. The effects of the operational parameters of furfural concentration (200–700 mg/L), initial pH (2–12), TiO_2/GAC composite dosage (1–3.5 g/L), and irradiation time (20–120 min) were studied. The synthetized TiO_2/GAC composite exhibited a total pore volume of 0.13 cm^3/g and specific surface area of 35.91 m^2/g. Removal efficiency of up to 95% was observed at initial pH of 10, TiO_2/GAC dosage of 2.5 g/L, irradiation time of 80 min, and initial furfural concentration of 500 mg/L. The photocatalyst could be reused at least four consecutive times with a mere 2% decrease in furfural removal efficiency. Mineralization efficiency of 94% was obtained within 80 min. Pseudo-first-order kinetics best fit the photocatalytic degradation of furfural under experimental conditions.

1. Introduction

Discharge of organic wastes such as furfural from petrochemical installations, oil refineries, and other chemical industrial plants into the environment is an important source of water pollution. Some of these organic compounds inhibit metabolism and are toxic to organisms [1, 2]. Furfural is an organic chemical and an excellent solvent used in oil extraction units and the petrochemical industry to separate hydrocarbons. Furfural is highly resistant and has a very slow speed of decomposition in the environment. Adsorption of furfural through the skin is toxic and harmful to the nervous system. The mechanism of furfural toxicity is a chemical reaction with internal cell components, damage to cell membranes, and prevention of cell metabolism [3–8]. Development of efficient treatments for the degradation and mineralization of furfural from effluents is essential [9, 10].

Photo-induced oxidation techniques have been increasingly studied for degradation of complex and recalcitrant organic chemicals. Heterogeneous photocatalysis is an advanced oxidation technique which oxidizes a range of organic compounds under ambient conditions. Photocatalysis is the integration of light irradiation with oxidizing agents and mineral catalysts [11–18].

Titanium dioxide (TiO_2) is a semiconductor which is a promising photocatalyst for degradation of recalcitrant organics. It offers excellent photocatalytic features, low toxicity, ease of access, strong oxidizing ability, stability, reusability, and ability to be immobilized on carbon and zeolite beds. TiO_2 exists mainly in anatase, rutile, and brookite crystalline forms, each exhibiting different physical properties and photochemical reactivity. Anatase TiO_2 exhibits higher photocatalytic activity than the rutile or brookite types; however, problems exist in the practical application of TiO_2 for photocatalytic degradation. These include difficulty of separation of TiO_2 from the treated solution, difficulty of application of particulate suspensions in continuous flows, and the tendency of suspended TiO_2 to aggregate, especially at high concentrations [19–33].

Immobilization of TiO_2 on a support material has been proposed to overcome these problems. Initially, studies focused on immobilization of TiO_2 on fixed supports such as glass fiber, quartz, glass, and stainless steel; however, the efficiency of photocatalysis usually decreases on such immobilized TiO_2 composites because of limitations in mass transfer [17]. In order to increase mass transfer, a suspension system is preferred that allows suitable contact between catalyst, light irradiation, and pollutant in an aqueous solution [17, 34].

TiO_2 immobilization on porous beds such as silica, alumina, zeolite, activated carbon, and LECA has been studied [3, 22, 32, 35–38]. The main features of a support material are high specific surface area to allow immobilization of a greater amount of catalyst and low density to allow fluidization of the catalyst.

Granular activated carbon (GAC) has a high specific area and low density, which makes it a suitable support for synthesis of TiO_2/GAC. Other advantages of GAC as a support are mitigation of toxic shock to the system by adequate adsorption of contaminants, increased production of radicals to aid degradation [39–42], and the ability of GAC to adsorb pollutants and release them onto the surface of the TiO_2. This forms a concentration gradient of pollution around the TiO_2 in the solution that will increase the degradation rate of the pollutants [43]. Intermediates produced during photocatalysis can be adsorbed by GAC and further oxidized, allowing removal of secondary pollutants produced during decomposition [44].

The current study examined immobilization of synthetized TiO_2 nanoparticles on GAC and the effect of initial pH, photocatalyst dosage, irradiation time, and furfural concentration on the degradation rate of furfural in an aqueous phase. The reusability of TiO_2/GAC composite, adsorption effect, and kinetics of reactions were also studied.

2. Materials and Methods

2.1. Materials. Titanium butoxide ($Ti(OC_4H_9)_4$, 97%), ethanol (C_2H_6O), furfural ($C_5H_4O_2$), acetyl acetone ($C_5H_8O_2$), granular activated carbon, hydrochloric acid (HCl), and sodium hydroxide (NaOH) were all of analytical grade (Merck, Germany). Raw TiO_2 (Degussa, Germany) was composed of 75% anatase and 25% rutile forms with a mean particle size of 25 nm and BET specific surface area of 48 m^2/g. The GAC was washed with deionized water and dried in an oven at 105°C. All chemicals were used as received without further purification and all solutions were prepared using deionized water.

2.2. TiO_2/GAC Composite Synthesis. The nanosized TiO_2/GAC composite was synthetized by the sol-gel method using tetra-n-butyl titanate ($C_{16}H_{36}O_4Ti$) as the precursor. For synthesis, 25 mL of $Ti(OC_4H_9)_4$ was dissolved in 100 mL ethanol and stirred for 1 h with a magnetic stirrer (1000 rpm) at room temperature. For hydrolysis of the sol, a solution containing 2 mL HCl (35%) and 1 mL deionized water was added dropwise while stirring. Following this, 2.5 mL of acetyl acetone was slowly added as a stabilizer and the solution was continuously stirred (1200 rpm) for 1 h under vigorous mixing until a clear transparent sol was obtained. Then, 15 g GAC was added, the temperature was adjusted to 80°C, and the system was stirred (500 rpm) for 4 h until the titanium sol/GAC became titanium gel/GAC. After aging for 36 h at room temperature, the gel was dried for 2 h at 105°C in an oven and then calcined at 500°C for 2 h [11, 19, 32].

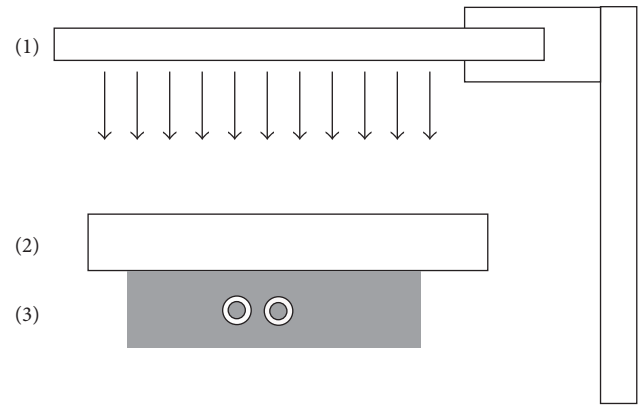

Figure 1: Schematic of fluidized bed photoreactor. (1) Adjustable UVC lamp. (2) Rectangular cubic reactor. (3) Magnetic stirrer.

2.3. Experimental Setup. Figure 1 is a schematic of the batch photoreactor. A rectangular cubic glass photoreactor with a total volume of 480 mL (4 cm × 4 cm × 30 cm) without the upper face was used. The light source comprised two 8 W UVC lamps installed above the reactor at a distance of 3 cm from the reactor edge. The reactor contents were mixed with an agitator system and 200 mL of synthetic wastewater was introduced to the photoreactor in all runs.

2.4. Photocatalytic Degradation. The photocatalytic degradation of furfural was performed in batch mode. Synthetic wastewater was prepared by the addition of the desired amounts of furfural to deionized water. Experiments were performed at ambient temperature and the pH of the solution was adjusted by addition of 0.1 N HCl and/or 0.1 N NaOH. The optimum conditions for initial pH (2, 4, 6, 8, 10, and 12), TiO_2/GAC composite dosage (1, 1.5, 2, 2.5, 3, and 3.5 g/L), irradiation time (20, 40, 60, 80, 100, and 120 min), and furfural concentration (200, 300, 400, 500, 600, and 700 mg/L) were studied consecutively. All experiments were carried out at room temperature at a constant stirring speed of 250 rpm. The furfural removal was determined using

$$\text{Removal efficiency } (\%) = \left(\frac{(\text{Furfural}_0 - \text{Furfural}_t)}{(\text{Furfural}_0)}\right) \times 100, \quad (1)$$

where furfural_0 and furfural_t denote furfural concentrations before and after the photocatalytic reaction, respectively.

TOC analysis was conducted to study mineralization. The degree of furfural mineralization in the photocatalytic processes can be calculated using

$$\text{Mineralization efficiency } (\%) = \left(\frac{(\text{TOC}_0 - \text{TOC}_t)}{(\text{TOC}_0)}\right) \times 100, \quad (2)$$

where TOC_0 and TOC_t denote the TOC concentrations before and after the reaction, respectively.

TOC was measured with a TOC analyzer (TOC-VCSH; Shimadzu, Japan). The effect of furfural adsorption on GAC was studied in the absence of light irradiation under the optimal conditions. To evaluate the feasibility of repeated use of TiO_2/GAC composite, four cycles of photocatalytic degradation of furfural were carried out under optimal conditions.

2.5. Analytical Methods. After a specified contact time, the reaction was terminated by turning off the UVC lamps. The photocatalysts were then separated and the furfural concentration was determined using a UV-vis spectrophotometer (DR 5000; Hach, USA) at λ_{max} = 277 nm. The crystallographic phase of the synthesized TiO_2 on the GAC sample was determined using a JNR (MPD300) X-ray diffractometer with a Cu anode at λ = 0.15060 nm, a voltage of 40 kV, and current intensity of 30 mA. The mean crystallite size was calculated using the Scherrer formula [45, 46]:

$$D = \frac{k\lambda}{\beta \cos\theta}, \quad (3)$$

where λ is the wavelength of X-ray radiation, k which is usually 0.89 is the Scherrer constant, λ = 1.5060 Å is the wavelength of the X-ray radiation, β is the peak full width at half maximum in radians, and θ is the Bragg diffraction angle. The specific surface area and pore volume of the samples were measured by nitrogen adsorption-desorption at 77 K using the BET method with a BELSORP-mini II (Bel, Japan). The micrographs of the TiO_2/GAC and original GAC were examined by field emission scanning electron microscopy (FESEM; Mira 3, Tescan).

3. Results and Discussion

3.1. Characterization of TiO_2/GAC Composite. It is commonly accepted that, in catalytic processes such as photocatalysis with crystalline TiO_2, the dispersion of the catalyst has a direct effect on catalytic efficiency [47]. A catalyst with finer particle sizes should, thus, produce higher activity during catalysis [48, 49]. The peaks in XRD analysis at 25.35°, 37.78°, 48.1°, 53.95°, 54.98°, 62.66°, 68.41°, and 74.91° are the diffraction values of (101), (004), (200), (105), (211), (204), (116), and (220) planes of the anatase form, which is in agreement with standard JCPDS card PDF 21-1272 (Figure 2). The peaks appearing at 20.96°, 50.23°, 60.02°, and 26.74° can be attributed to SiO_2, which is in good agreement with standard JCPDS card PDF 5-490. The results of XRD

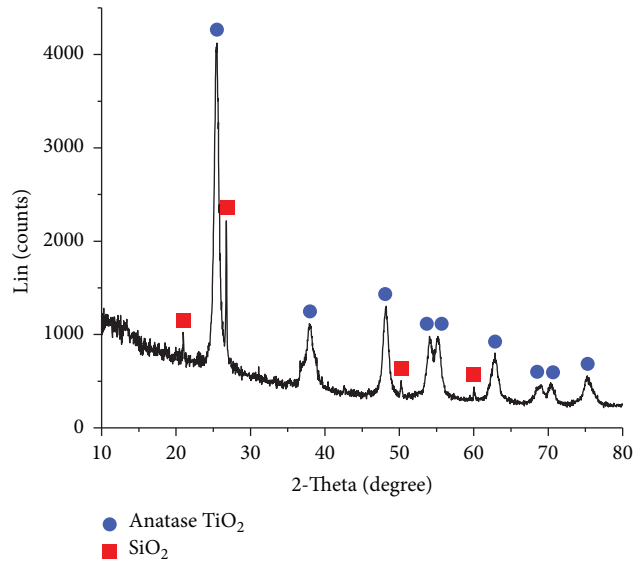

Figure 2: The XRD pattern of TiO_2/GAC composite.

indicate that the synthetized TiO_2 existed in an anatase state and there were no peaks that could be attributed to the brookite or rutile forms. Because of the existence of oxidizing solution and calcination at high temperatures, the silicon in the GAC structure oxidized and turned to SiO_2. The high performance of photocatalysis observed in this study for TiO_2/GAC composite suggests that a certain amount of crystalline phase TiO_2 nanoparticles was loaded with a high degree of dispersion onto the surface of the GAC. The average grain size of nanoparticles was estimated using Debye Scherrer's equation based on the full width at half maximum (FWHM) of the (101) peak of the composite. It was 21.4 nm.

Xue et al. synthesized TiO_2 in an anatase state on activated carbon and did not observe a brookite or rutile phase. They calcined TiO_2/GAC at 500°C [19]. Yao et al. synthesized TiO_2 nanoparticles on activated carbon fiber and studied the effect of calcination temperature. They observed an anatase state for TiO_2 at a calcination temperature of 500°C [32].

The TiO_2/GAC composite was sputter-coated with gold and examined by FESEM. Figure 3(a) shows the electron micrograph of the surface of raw GAC and Figure 3(b) of the surface of the TiO_2/GAC composite. The surface of the raw GAC is heterogeneous and grainy. Comparison of the GAC and TiO_2/GAC composite indicates that the TiO_2 nanoparticles fixed on the surface of GAC uniformly and the morphology of the surface of the GAC was modified after coating with TiO_2.

The particle size of the TiO_2 nanoparticles was 15–25 nm. This was caused by the high surface area of the GAC matrix, which favored a high degree of dispersion of TiO_2 nanoparticles. As expected, TiO_2 particles were deposited onto the surface and the mesopores and macropores of the GAC. TiO_2 on the surface had a greater chance to receive light irradiation and exhibited higher photocatalytic activity. Moussavi et al. used GAC as a support for synthesis of MgO/GAC composites and observed that the MgO nanocrystals were

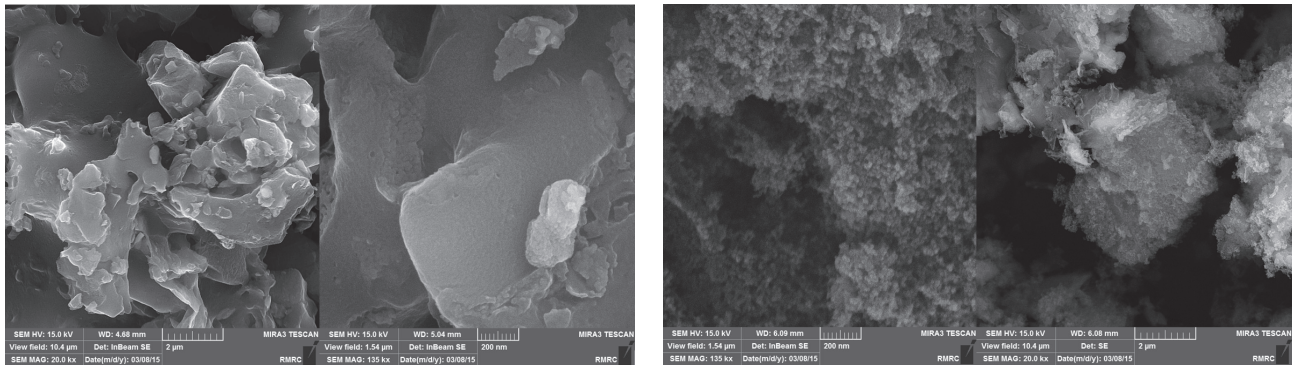

(a) (b)

Figure 3: (a) Electron micrograph of the surface of raw GAC. (b) Electron micrograph of the surface of the TiO_2/GAC composite.

Table 1: Characteristics of GAC and the TiO_2/GAC composite.

Parameter	Value	
	GAC	TiO_2/GAC
BET (m^2/g)	226.78	35.91
Total pore volume (cm^3/g)	0.182	0.130
Average pore diameter (nm)	3.22	14
BET constant	146	95

uniformly fixed onto the surface of the GAC and that the surface morphology of the GAC was noticeably modified after being coated with MgO [50]. Zhang et al. synthesized TiO_2/activated carbon using the AP-MOCVD method. They observed that the AC was covered with TiO_2 particles [43].

The nitrogen adsorption isotherms for the TiO_2/GAC composite and GAC are shown in Figure 4. The BET surface areas of GAC and TiO_2/GAC were 226.78 and 35.91 m^2/g, respectively. The total pore volume of the TiO_2/GAC composite was lower than that of the GAC, which decreased from 0.18 to 0.13 cm^3/g, indicating that some pores were blocked by the TiO_2 film (Table 1). The increase in average pore diameter of TiO_2/GAC composite to the GAC can be attributed to calcination at 500°C. These results are in accordance with the results of other researchers [19, 32, 51].

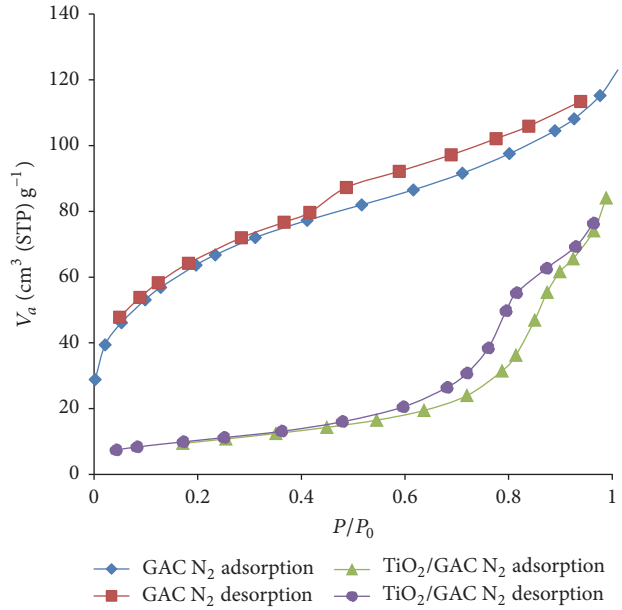

Figure 4: Nitrogen adsorption isotherms for the TiO_2/GAC composite and GAC.

3.2. Photocatalytic Degradation of Furfural

3.2.1. Effect of Initial pH. The results indicate that initial solution pH of up to 10 increased furfural degradation and higher values adversely affected removal efficiency (Figure 5). At acidic pH values, a high amount of conjugated base was added to the solution. The anion Cl^- reacted with hydroxyl radicals and formed inorganic radical ions (ClO^-). These inorganic radical anions showed much lower reactivity than the hydroxyl radicals ($OH^\bullet$) and did not participate in the degradation of furfural. There was also intense competition between furfural molecules and anions for $OH^\bullet$ [52, 53]. An increase in OH^- and its reaction with the positive holes (h_{vb}^+) on the surface of the TiO_2 in the composite increased $OH^\bullet$ production. The hydroxyl radical was an extremely strong, nonselective oxidant (E^0 = +3.06 V) which caused partial or complete mineralization of furfural. More efficient formation of hydroxyl radicals occurred in an alkaline solution and increased degradation efficiency [54, 55].

A decrease in degradation efficiency of furfural occurred at initial pH values above 10. At a high concentration of OH^- (pH > 10), two mechanisms may cause deactivation of $OH^\bullet$. First, $H_2O_2^\bullet$ and $HO_2^\bullet$ radicals form in the reaction of OH with OH^-, but the reactivity of these radicals with organic materials is less than with $OH^\bullet$ [52, 53]. Second, the presence of high amounts of hydroxyl radicals causes radical-radical reactions at higher pH values and leads to a scavenging effect on $OH^\bullet$ [56]. These results are in accordance with the results of Mousavi-Mortazavi and Nezamzadeh-Ejhieh in which they observed the same results for furfural degradation using FeO-clinoptilolite [3]. Shavisi et al. also

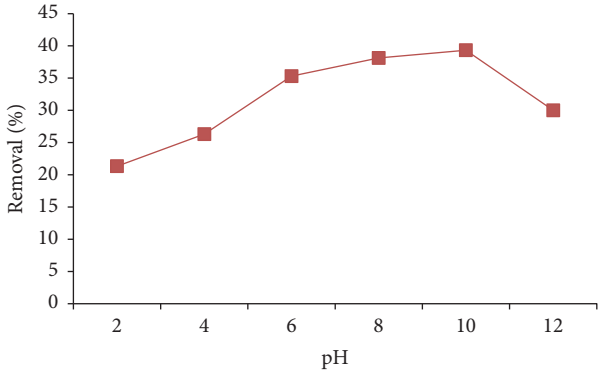

Figure 5: Effect of pH on degradation of furfural. TiO_2/GAC composite dosage: 1.5 g/L, irradiation time: 40 min, and initial furfural concentration: 300 mg/L.

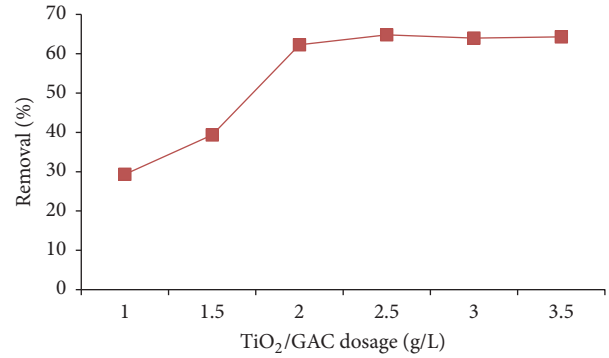

Figure 6: Effect of TiO_2/GAC composite dosage on the degradation of furfural. Irradiation time: 40 min, initial furfural concentration: 300 mg/L, and initial pH: 10.

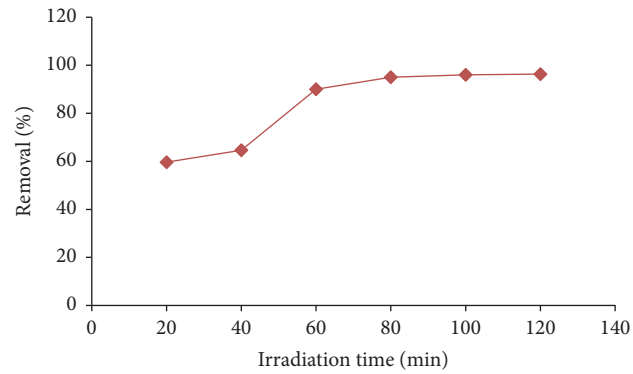

Figure 7: Effect of irradiation time on the degradation of furfural. TiO_2/GAC composite dosage: 2.5 g/L, initial pH: 10, and initial furfural concentration: 300 mg/L.

observed similar results for degradation of ammonia in petrochemical wastewater using TiO_2/LECA photocatalyst. They recorded their best degradation efficiency at pH = 10; however, they justified these results on the basis of the zero point charge of TiO_2 [38].

3.2.2. Effect of TiO_2/GAC Dosage. During photocatalytic degradation, the catalyst dosage is important and the optimum catalyst dosage must be determined to avoid the use of excess catalyst for efficient degradation of furfural in aqueous solutions. The catalyst dosage has both positive and negative impacts on the photodegradation rate. An increase in the amount of active sites on the catalyst surface increases the interaction between the photocatalyst and the furfural molecules or deactivates them by combining them to form a dense layer of catalyst [40, 54, 55, 57]. With an increase in catalyst dosage up to 2.5 g/L, photon absorption increased, which increased the degradation rate. The addition of catalyst beyond 2.5 g/L resulted in the deactivation of activated molecules in suspension through collision with other molecules. This means that as the amount of catalyst increased, UVC-activated molecules collided with the excess catalyst that eventually caused their deactivation as shown in

$$\mathrm{TiO_2}^{*}/\mathrm{GAC} + \mathrm{TiO_2}/\mathrm{GAC} \longrightarrow \mathrm{TiO_2}^{\#}/\mathrm{GAC} + \mathrm{TiO_2}/\mathrm{GAC} \quad (4)$$

where $TiO_2{}^{*}$/GAC represents the catalyst with active species and $TiO_2{}^{\#}$/GAC represents the deactivated form of the catalyst.

Aggregation (particle-particle interaction) began at photocatalyst dosages of >2.5 g/L and reduced the effective surface area of the catalyst and adsorption of the reactants. The results clearly indicate that an increase in photocatalyst concentration from 1 to 2.5 g/L increased furfural removal from 29.33% to 64.8% during the 40 min irradiation time (Figure 6). Increasing the catalyst dosage increased turbidity of the suspension and UV light penetration decreased as a result of the increased scattering effect, decreasing photoactivation efficiency [58–60]. Because the most effective removal of furfural was observed at 2.5 g/L TiO_2/GAC, further testing was carried out at this dosage.

3.2.3. Effect of Irradiation Time. Furfural removal increased significantly as UV irradiation time increased but remained almost unchanged after 80 min of irradiation (Figure 7). The removal efficiency of furfural increased with an increase in $OH^{\bullet}$ generation as more UV light irradiation became available [11]. An optimum irradiation time of 80 min was, thus, selected.

3.2.4. Effect of Initial Furfural Concentration. Furfural removal efficiency decreased from 98.5% to 85.42% as initial furfural concentration increased from 200 to 700 mg/L (Figure 8). This indicates that as the initial furfural concentration increased, molecule adsorption on the surface of the TiO_2/GAC increased. The high amount of contaminants adsorbed onto the surface of the composite inhibited the reaction of furfural molecules with the photogenerated holes and hydroxyl radicals by preventing direct contact between them. An increase in contaminant concentration caused the furfural molecules to absorb UV rays and the photons never reach the photocatalyst surface; thus, photocatalytic degradation efficiency decreased [12, 61]. Faramarzpour et

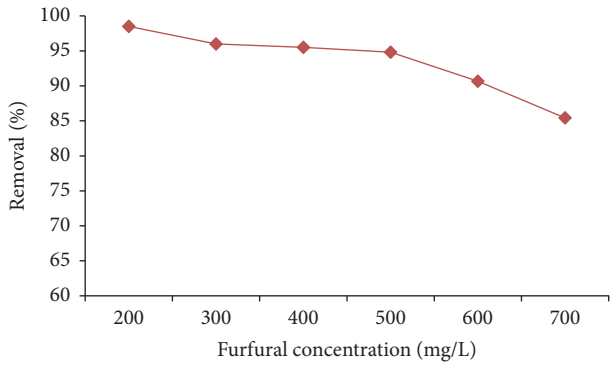

Figure 8: Effect of initial furfural concentration on the photocatalytic degradation of furfural. TiO_2/GAC composite dosage: 2.5 g/L, irradiation time: 80 min, and initial pH: 10.

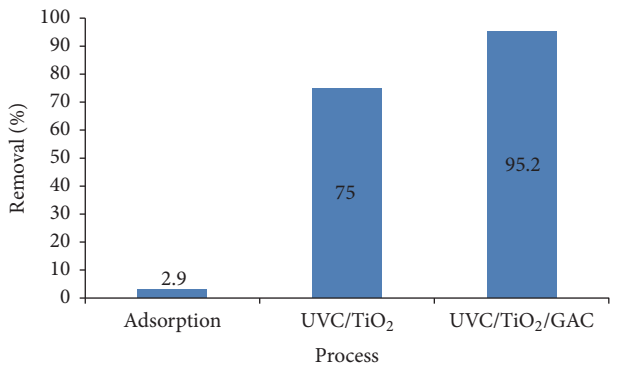

Figure 9: Comparison of the furfural removal efficiency in adsorption, UVC/TiO_2, and UVC/TiO_2/GAC processes at the same operational conditions irradiation, time = 80 min, photocatalyst dosage = 2.5 g/L, initial furfural concentration = 500 mg/L, and initial pH = 10.

Table 2: The cyclic photocatalytic performance of TiO_2/GAC composite for furfural degradation with furfural concentration = 500 mg/L, initial pH = 10, photocatalyst dosage = 2.5 g/L, and irradiation time of 80 min.

Number of cyclic usage	Degradation efficiency %
First cycle	95.2
Second cycle	94.6
Third cycle	94.2
Fourth cycle	93.4

al. observed similar results for degradation of furfural using TiO_2/perlite photocatalyst [62].

3.3. Reusability of TiO_2/GAC Composite. To evaluate the feasibility of repeated use of TiO_2/GAC photocatalyst, four cycles of photocatalytic degradation of furfural were carried out as shown in Table 2. The degradation efficiency of furfural over the four cycles indicated that the photocatalytic activity remained at about 93% for an irradiation time of 80 min. Removal in the first cycle was 95.2%; thus, furfural removal efficiency decreased by only about 2% over the four cycles. This very small decrease resulted from the slight dislodging of TiO_2 from the GAC under stirring or from the decrease in adsorption capacity and active sites on the reused photocatalyst.

Shavisi et al. observed a decrease in efficiency of photocatalysis after each reuse to be about 14%. They attributed this to the decrease in adsorption capacity and active sites on reused catalyst. They experienced about a 41% decrease in catalyst efficiency after three regenerations and usages. Their photocatalyst was TiO_2/LECA [38].

It appears that the anatase TiO_2 firmly attached to the GAC surface and could not be easily exfoliated under mechanical stirring of the solutions. It is also shown that the final removal of organic pollutant from solution is caused by photocatalytic degradation rather than by adsorption, as adsorption would undoubtedly result in saturation of the organic pollutant on the photocatalyst. Yao et al. attained 87% degradation efficiency of methyl orange at an irradiation time of 2 h and 83.58% degradation efficiency of phenol at an irradiation time of 4 h after four cycles of TiO_2/ACF [32].

3.4. Adsorption Effect. To investigate the effect of adsorption, one experiment was performed under optimum conditions without UV irradiation. A degradation efficiency of 2.6% (Figure 9) indicated that the influence of adsorption was very low and that photocatalysis was the main mechanism in furfural removal.

3.5. Photocatalytic Degradation of Furfural through UVC/TiO_2. The influence of UVC/TiO_2 under optimum conditions was compared with TiO_2/GAC composite. A degradation efficiency of 75% was observed using TiO_2 as a photocatalyst (Figure 9) and indicates that the efficiency of photocatalysis when GAC is used as a support increases and successfully solves the problems associated with raw TiO_2.

TiO_2 dispersion on the surface of the GAC decreases TiO_2 agglomeration and increases the effective surface area of the TiO_2 nanoparticles which in turn increases the formation of hydroxyl radicals. In addition, GAC has a good adsorption ability and the organic pollutant adsorbs to TiO_2/GAC composite and enhances the probability of degradation. Hence, integration of the photocatalytic activity with the adsorption capacity of GAC in the supported TiO_2 induces a synergistic effect, causing a considerable enhancement in the photocatalytic activity [63].

3.6. Mineralization of Furfural. TOC was measured under optimum conditions to determine the mineralization rate. TOC removal of 94% was observed and nearly complete mineralization was observed within 80 min. It can be deduced that the furfural experienced nearly complete mineralization into CO_2 and H_2O and that most intermediate products degraded during the process.

3.7. Mechanism of Photocatalytic Degradation. The mechanism of decomposition of organic pollutants catalyzed by TiO_2 follows three main stages: (1) movement of pollutant

from the liquid bulk to the catalyst surface; (2) adsorption of organic pollutants onto the surface of the TiO_2/GAC composite; (3) photodegradation of organic pollutants onto the surface of the composite; (4) movement of the final products from the surface of TiO_2/GAC composite to the bulk of solution. The photodegradation of organic pollutants is the step that involves direct charge transfer from the semiconductor to the organic pollutants adsorbed at the active TiO_2/GAC spots.

Under UV irradiation, TiO_2 nanoparticles on the surface of the GAC and in the porous structure of the GAC react with the UV light to produce electrons (e_{cb}) and holes (h_{vb}^+). The holes are trapped by H_2O or O_2 on the surface of the TiO_2 nanoparticle to yield H^+ and $OH^\bullet$ radicals, an efficient oxidizing agent for decomposition of organic components. Generally, in semiconductor photocatalysis, photon-generated holes (h_{vb}^+), electrons (e_{cb}), superoxide ions ($O_2^{\bullet-}$), and hydroxyl radicals ($OH^\bullet$) take part in redox reactions if thermodynamically favorable. h_{vb}^+, e_{cb}, $OH^\bullet$, and $O_2^{\bullet-}$ can thus degrade the organic pollutant into intermediates and the intermediates can be further degraded into CO_2 and H_2O. In the current study, the degradation of furfural is proposed to follow this path [19, 44, 64, 65]:

$$TiO_2 + UV \longrightarrow h^+ (VB) + e^- (CB) \quad (5)$$

$$h^+ (VB) + OH^- \longrightarrow OH^\bullet \quad (6)$$

$$e^- (CB) + O_2 \longrightarrow O_2^{\bullet-} \quad (7)$$

$$O_2^{\bullet-} + e^- (CB) + H^+ \longrightarrow H_2O_2 \quad (8)$$

$$O_2^{\bullet-} + O_2^{\bullet-} + 2H^+ \longrightarrow H_2O_2 + O_2 \quad (9)$$

$$H_2O_2 + e^- (CB) \longrightarrow OH^\bullet + OH^- \quad (10)$$

$$\text{Furfural} + OH^\bullet \longrightarrow H_2O + CO_2 + \text{other degradation products} \quad (11)$$

$$\text{Furfural} + O_2^{\bullet-} \longrightarrow H_2O + CO_2 + \text{other degradation products} \quad (12)$$

3.8. Kinetic Study. The Langmuir–Hinshelwood model is usually applied to describe the kinetics of photocatalytic reactions in aqueous solutions for catalytic degradation of organic compounds through adsorption [66, 67]. The model relates the rate of photodegradation (r) and the concentration of furfural (C) and is expressed as

$$r = -\frac{dC}{dt} = \frac{(k_r K_{ad} C)}{(1 + K_{ad} C)}, \quad (13)$$

where k_r is the intrinsic rate constant (M/min), K_{ad} is the adsorption equilibrium constant of furfural on a catalyst particle (M^{-1}), and t is the irradiation time (min). When adsorption is rather weak, (13) can be simplified into (14)

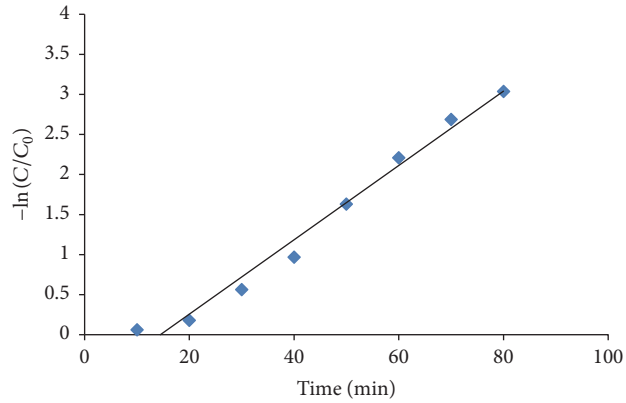

Figure 10: Pseudo-first-order plot for the photocatalytic degradation of furfural; TiO_2/GAC composite dosage = 2.5 g/L, initial furfural concentration = 500 mg/L, and initial pH = 10.

for pseudo-first-order kinetics with an apparent rate constant k_{app} (min^{-1}):

$$\ln\left(\frac{C}{C_0}\right) = -k_r K_{ad} t = -k_{app} t. \quad (14)$$

If pseudo-first-order kinetics are applicable, the plot of $-\ln(C/C_0)$ against t should yield a straight line, as indicated in (14), from which k_{app} can be obtained from the slope of the plot [67, 68]. Figure 10 shows that the pseudo-first-order kinetic model adequately fits the experimental data (R^2 = 0.98) with k_{app} of 0.046 min^{-1}.

4. Conclusions

The present study revealed that photocatalysis with TiO_2/GAC composite could be applied for treatment of effluent containing furfural. Experiments indicated that photocatalytic degradation of furfural using UVC/TiO_2/GAC was feasible and that pseudo-first-order kinetics successfully described the photocatalytic degradation behavior. Under optimal operational conditions, furfural removal was 95%. Anatase TiO_2 was firmly attached to the granular activated carbon surface that could not to be easily exfoliated from the granular carbon with mechanical stirring of the solutions. Results indicated that furfural removal due to only physical adsorption on GAC was low and photocatalytic removal of furfural was efficiently promoted when GAC was used as a support. TiO_2 dispersion on the surface of the GAC decreased TiO_2 agglomeration and increased the effective surface area of the TiO_2 nanoparticles which in turn increased the formation of hydroxyl radicals and caused enhancement of photocatalytic degradation of furfural using TiO_2/GAC composite.

Competing Interests

The authors declare that they have no competing interests.

Acknowledgments

The authors thank the Petroleum University of Technology and Ahvaz Jundishapur University of Medical Sciences for financial and other supports.

References

[1] S. M. Borghei and S. N. Hosseini, "Comparison of furfural degradation by different photooxidation methods," *Chemical Engineering Journal*, vol. 139, no. 3, pp. 482–488, 2008.

[2] U. K. Ghosh, N. C. Pradhan, and B. Adhikari, "Pervaporative separation of furfural from aqueous solution using modified polyurethaneurea membrane," *Desalination*, vol. 252, no. 1-3, pp. 1–7, 2010.

[3] S. Mousavi-Mortazavi and A. Nezamzadeh-Ejhieh, "Supported iron oxide onto an Iranian clinoptilolite as a heterogeneous catalyst for photodegradation of furfural in a wastewater sample," *Desalination and Water Treatment*, vol. 57, no. 23, pp. 10802–10814, 2016.

[4] M. Anbia and N. Mohammadi, "A nanoporous adsorbent for removal of furfural from aqueous solutions," *Desalination*, vol. 249, no. 1, pp. 150–153, 2009.

[5] P. Gupta, A. Nanoti, M. O. Garg, and A. N. Goswami, "The removal of furfural from water by adsorption with polymeric resins," *Separation Science and Technology*, vol. 36, no. 13, pp. 2835–2844, 2001.

[6] A. K. Sahu, I. D. Mall, and V. C. Srivastava, "Studies on the adsorption of furfural from aqueous solution onto low-cost bagasse fly ash," *Chemical Engineering Communications*, vol. 195, no. 3, pp. 316–335, 2007.

[7] K. E. Manz, G. Haerr, J. Lucchesi, and K. E. Carter, "Adsorption of hydraulic fracturing fluid components 2-butoxyethanol and furfural onto granular activated carbon and shale rock," *Chemosphere*, vol. 164, pp. 585–592, 2016.

[8] M. Cuevas, S. M. Quero, G. Hodaifa, A. J. M. López, and S. Sánchez, "Furfural removal from liquid effluents by adsorption onto commercial activated carbon in a batch heterogeneous reactor," *Ecological Engineering*, vol. 68, pp. 241–250, 2014.

[9] C.-L. Kang, X.-J. Tang, X.-Q. Jiao, P. Guo, F.-M. Quan, and X.-Y. Lin, "Degradation of furfural by UV/O_3 technology," *Chemical Research in Chinese Universities*, vol. 25, no. 4, pp. 451–454, 2009.

[10] Y.-H. Shih and M.-Y. Chen, "Effect of cations on degradation of pentachlorophenol by nanoscale Pd/Fe bimetallic particles," *Sustainable Environment Research*, vol. 20, no. 5, pp. 333–339, 2010.

[11] B. Zhu and L. Zou, "Trapping and decomposing of color compounds from recycled water by TiO_2 coated activated carbon," *Journal of Environmental Management*, vol. 90, no. 11, pp. 3217–3225, 2009.

[12] R.-P. Qiao, N. Li, X.-H. Qi, Q.-S. Wang, and Y.-Y. Zhuang, "Degradation of microcystin-RR by UV radiation in the presence of hydrogen peroxide," *Toxicon*, vol. 45, no. 6, pp. 745–752, 2005.

[13] P. Palaniandy, H. Bin, A. Aziz, and S. Feroz, "Evaluating the TiO_2 as a solar photocatalyst process by response surface methodology to treat the petroleum waste water," *Karbala International Journal of Modern Science*, vol. 1, no. 2, pp. 78–85, 2015.

[14] I. T. Peternel, N. Koprivanac, A. M. L. Božić, and H. M. Kušić, "Comparative study of UV/TiO_2, UV/ZnO and photo-Fenton processes for the organic reactive dye degradation in aqueous solution," *Journal of Hazardous Materials*, vol. 148, no. 1-2, pp. 477–484, 2007.

[15] L. Bilińska, M. Gmurek, and S. Ledakowicz, "Comparison between industrial and simulated textile wastewater treatment by AOPs—biodegradability, toxicity and cost assessment," *Chemical Engineering Journal*, vol. 306, pp. 550–559, 2016.

[16] H. Kusic, D. Juretic, N. Koprivanac, V. Marin, and A. L. Božić, "Photooxidation processes for an azo dye in aqueous media: modeling of degradation kinetic and ecological parameters evaluation," *Journal of Hazardous Materials*, vol. 185, no. 2-3, pp. 1558–1568, 2011.

[17] N. J. Peill and M. R. Hoffmann, "Chemical and physical characterization of a TiO_2-coated fiber optic cable reactor," *Environmental Science and Technology*, vol. 30, no. 9, pp. 2806–2812, 1996.

[18] M. M. Bello, A. A. Abdul Raman, and M. Purushothaman, "Applications of fluidized bed reactors in wastewater treatment—a review of the major design and operational parameters," *Journal of Cleaner Production*, vol. 141, pp. 1492–1514, 2017.

[19] G. Xue, H. Liu, Q. Chen, C. Hills, M. Tyrer, and F. Innocent, "Synergy between surface adsorption and photocatalysis during degradation of humic acid on TiO_2/activated carbon composites," *Journal of Hazardous Materials*, vol. 186, no. 1, pp. 765–772, 2011.

[20] H. F. Moafi, "Photocatalytic self-cleaning properties of lanthanum and silver co-doped TiO_2 nanocomposite on polymeric fibers," *Iranian Journal of Catalysis*, vol. 6, no. 3, pp. 281–292, 2016.

[21] A. Bahranifard, "Application of TiO_2-zeolite as photocatalyst for photodegradation of some organic pollutants," *Iranian Journal of Catalysis*, vol. 1, no. 1, pp. 45–50, 2011.

[22] H. Zabihi-Mobarakeh and A. Nezamzadeh-Ejhieh, "Application of supported TiO_2 onto Iranian clinoptilolite nanoparticles in the photodegradation of mixture of aniline and 2, 4-dinitroaniline aqueous solution," *Journal of Industrial and Engineering Chemistry*, vol. 26, pp. 315–321, 2015.

[23] A. Nezamzadeh-Ejhieh and M. Bahrami, "Investigation of the photocatalytic activity of supported ZnO-TiO_2 on clinoptilolite nano-particles towards photodegradation of wastewater-contained phenol," *Desalination and Water Treatment*, vol. 55, no. 4, pp. 1096–1104, 2015.

[24] D. Nguyen Thanh, O. Kikhtyanin, R. Ramos et al., "Nanosized TiO_2—a promising catalyst for the aldol condensation of furfural with acetone in biomass upgrading," *Catalysis Today*, vol. 277, pp. 97–107, 2016.

[25] E. Bailón-García, A. Elmouwahidi, M. A. Álvarez, F. Carrasco-Marín, A. F. Pérez-Cadenas, and F. J. Maldonado-Hódar, "New carbon xerogel-TiO_2 composites with high performance as visible-light photocatalysts for dye mineralization," *Applied Catalysis B: Environmental*, vol. 201, pp. 29–40, 2017.

[26] A. L. Linsebigler, G. Lu, and J. T. Yates Jr., "Photocatalysis on TiO_2 surfaces: principles, mechanisms, and selected results," *Chemical Reviews*, vol. 95, no. 3, pp. 735–758, 1995.

[27] M. R. Hoffmann, S. T. Martin, W. Choi, and D. W. Bahnemann, "Environmental applications of semiconductor photocatalysis," *Chemical Reviews*, vol. 95, no. 1, pp. 69–96, 1995.

[28] I. Sopyan, M. Watanabe, S. Murasawa, K. Hashimoto, and A. Fujishima, "An efficient TiO_2 thin-film photocatalyst: photocatalytic properties in gas-phase acetaldehyde degradation,"

Journal of Photochemistry and Photobiology A: Chemistry, vol. 98, no. 1-2, pp. 79–86, 1996.

[29] H. Cao, S. Huang, Y. Yu, Y. Yan, Y. Lv, and Y. Cao, "Synthesis of TiO_2-N/SnO_2 heterostructure photocatalyst and its photocatalytic mechanism," *Journal of Colloid and Interface Science*, vol. 486, pp. 176–183, 2017.

[30] R. Thiruvenkatachari, S. Vigneswaran, and I. S. Moon, "A review on UV/TiO_2 photocatalytic oxidation process," *Korean Journal of Chemical Engineering*, vol. 25, no. 1, pp. 64–72, 2008.

[31] K.-H. Wang, Y.-H. Hsieh, M.-Y. Chou, and C.-Y. Chang, "Photocatalytic degradation of 2-chloro and 2-nitrophenol by titanium dioxide suspensions in aqueous solution," *Applied Catalysis B: Environmental*, vol. 21, no. 1, pp. 1–8, 1999.

[32] S. Yao, J. Li, and Z. Shi, "Immobilization of TiO_2 nanoparticles on activated carbon fiber and its photodegradation performance for organic pollutants," *Particuology*, vol. 8, no. 3, pp. 272–278, 2010.

[33] X. Tang, Q. Feng, K. Liu, and Y. Tan, "Synthesis and characterization of a novel nanofibrous TiO_2/SiO_2 composite with enhanced photocatalytic activity," *Materials Letters*, vol. 183, pp. 175–178, 2016.

[34] A. Fernández, G. Lassaletta, V. M. Jiménez et al., "Preparation and characterization of TiO_2 photocatalysts supported on various rigid supports (glass, quartz and stainless steel). Comparative studies of photocatalytic activity in water purification," *Applied Catalysis B, Environmental*, vol. 7, no. 1-2, pp. 49–63, 1995.

[35] L. J. Alemany, M. A. Bañares, E. Pardo, F. Martin, M. Galán-Fereres, and J. M. Blasco, "Photodegradation of phenol in water using silica-supported titania catalysts," *Applied Catalysis B: Environmental*, vol. 13, no. 3-4, pp. 289–297, 1997.

[36] W. Huang, A. Duan, Z. Zhao et al., "Ti-modified alumina supports prepared by sol-gel method used for deep HDS catalysts," *Catalysis Today*, vol. 131, no. 1–4, pp. 314–321, 2008.

[37] S. Fukahori, H. Ichiura, T. Kitaoka, and H. Tanaka, "Photocatalytic decomposition of bisphenol A in water using composite TiO_2-zeolite sheets prepared by a papermaking technique," *Environmental Science and Technology*, vol. 37, no. 5, pp. 1048–1051, 2003.

[38] Y. Shavisi, S. Sharifnia, M. Zendehzaban, M. L. Mirghavami, and S. Kakehazar, "Application of solar light for degradation of ammonia in petrochemical wastewater by a floating TiO_2/LECA photocatalyst," *Journal of Industrial and Engineering Chemistry*, vol. 20, no. 5, pp. 2806–2813, 2014.

[39] J. Nawrocki and B. Kasprzyk-Hordern, "The efficiency and mechanisms of catalytic ozonation," *Applied Catalysis B: Environmental*, vol. 99, no. 1-2, pp. 27–42, 2010.

[40] P. C. C. Faria, J. J. M. Órfão, and M. F. R. Pereira, "Activated carbon and ceria catalysts applied to the catalytic ozonation of dyes and textile effluents," *Applied Catalysis B: Environmental*, vol. 88, no. 3-4, pp. 341–350, 2009.

[41] J. Araña, J. M. Doña-Rodríguez, E. Tello Rendón et al., "TiO_2 activation by using activated carbon as a support: Part II. Photoreactivity and FTIR study," *Applied Catalysis B: Environmental*, vol. 44, no. 2, pp. 153–160, 2003.

[42] B. Kasprzyk-Hordern, M. Ziółek, and J. Nawrocki, "Catalytic ozonation and methods of enhancing molecular ozone reactions in water treatment," *Applied Catalysis B: Environmental*, vol. 46, no. 4, pp. 639–669, 2003.

[43] X. Zhang, M. Zhou, and L. Lei, "Preparation of photocatalytic TiO_2 coatings of nanosized particles on activated carbon by AP-MOCVD," *Carbon*, vol. 43, no. 8, pp. 1700–1708, 2005.

[44] H. Yoneyama and T. Torimoto, "Titanium dioxide/adsorbent hybrid photocatalysts for photodestruction of organic substances of dilute concentrations," *Catalysis Today*, vol. 58, no. 2, pp. 133–140, 2000.

[45] M. Bordbar, S. M. Vasegh, S. Jafari, and A. Y. Faal, "Optical and photocatalytic properties undoped and Mn-doped ZnO nanoparticles synthesized by hydrothermal method: effect of annealingtemperature," *Iranian Journal of Catalysis*, vol. 5, no. 2, pp. 135–141, 2015.

[46] P. Mohammadyari and A. Nezamzadeh-Ejhieh, "Supporting of mixed ZnS–NiS semiconductors onto clinoptilolite nanoparticles to improve its activity in photodegradation of 2-nitrotoluene," *RSC Advances*, vol. 5, no. 92, pp. 75300–75310, 2015.

[47] P. V. Nidheesh and R. Gandhimathi, "Trends in electro-Fenton process for water and wastewater treatment: an overview," *Desalination*, vol. 299, pp. 1–15, 2012.

[48] D. Wang, L. Xiao, Q. Luo, X. Li, J. An, and Y. Duan, "Highly efficient visible light TiO_2 photocatalyst prepared by sol–gel method at temperatures lower than 300 °C," *Journal of Hazardous Materials*, vol. 192, no. 1, pp. 150–159, 2011.

[49] J. Przepiórski, N. Yoshizawa, and Y. Yamada, "Activated carbons containing TiO_2: characterization and influence of a preparation method on the state of TiO_2 supported," *Journal of Materials Science*, vol. 36, no. 17, pp. 4249–4257, 2001.

[50] G. Moussavi, A. A. Aghapour, and K. Yaghmaeian, "The degradation and mineralization of catechol using ozonation catalyzed with MgO/GAC composite in a fluidized bed reactor," *Chemical Engineering Journal*, vol. 249, pp. 302–310, 2014.

[51] S. H. Yao, Y. F. Jia, and S. L. Zhao, "Photocatalytic oxidation and removal of arsenite by titanium dioxide supported on granular activated carbon," *Environmental Technology*, vol. 33, no. 9, pp. 983–988, 2012.

[52] A. Nezamzadeh-Ejhieh and S. Moeinirad, "Heterogeneous photocatalytic degradation of furfural using NiS-clinoptilolite zeolite," *Desalination*, vol. 273, no. 2-3, pp. 248–257, 2011.

[53] M. B. Kasiri, H. Aleboyeh, and A. Aleboyeh, "Degradation of Acid Blue 74 using Fe-ZSM5 zeolite as a heterogeneous photo-Fenton catalyst," *Applied Catalysis B: Environmental*, vol. 84, no. 1-2, pp. 9–15, 2008.

[54] N. Daneshvar, D. Salari, and A. R. Khataee, "Photocatalytic degradation of azo dye acid red 14 in water on ZnO as an alternative catalyst to TiO_2," *Journal of Photochemistry and Photobiology A: Chemistry*, vol. 162, no. 2-3, pp. 317–322, 2004.

[55] N. Daneshvar, M. H. Rasoulifard, A. R. Khataee, and F. Hosseinzadeh, "Removal of C.I. Acid Orange 7 from aqueous solution by UV irradiation in the presence of ZnO nanopowder," *Journal of Hazardous Materials*, vol. 143, no. 1-2, pp. 95–101, 2007.

[56] S. S. Ashraf, M. A. Rauf, and S. Alhadrami, "Degradation of Methyl Red using Fenton's reagent and the effect of various salts," *Dyes and Pigments*, vol. 69, no. 1-2, pp. 74–78, 2006.

[57] Z. M. El-Bahy, M. M. Mohamed, F. I. Zidan, and M. S. Thabet, "Photo-degradation of acid green dye over Co–ZSM-5 catalysts prepared by incipient wetness impregnation technique," *Journal of Hazardous Materials*, vol. 153, no. 1-2, pp. 364–371, 2008.

[58] N. Sobana and M. Swaminathan, "The effect of operational parameters on the photocatalytic degradation of acid red 18 by ZnO," *Separation and Purification Technology*, vol. 56, no. 1, pp. 101–107, 2007.

[59] M. Zendehzaban, S. Sharifnia, and S. N. Hosseini, "Photocatalytic degradation of ammonia by light expanded clay aggregate

(LECA)-coating of TiO_2 nanoparticles," *Korean Journal of Chemical Engineering*, vol. 30, no. 3, pp. 574–579, 2013.

[60] C. Chen, J. Liu, P. Liu, and B. Yu, "Investigation of photocatalytic degradation of methyl orange by using nano-sized ZnO catalysts," *Advances in Chemical Engineering and Science*, vol. 1, no. 1, pp. 9–14, 2011.

[61] S. Chakrabarti and B. K. Dutta, "Photocatalytic degradation of model textile dyes in wastewater using ZnO as semiconductor catalyst," *Journal of Hazardous Materials*, vol. 112, no. 3, pp. 269–278, 2004.

[62] M. Faramarzpour, M. Vossoughi, and M. Borghei, "Photocatalytic degradation of furfural by titania nanoparticles in a floating-bed photoreactor," *Chemical Engineering Journal*, vol. 146, no. 1, pp. 79–85, 2009.

[63] J. Esmaili-Hafshejani and A. Nezamzadeh-Ejhieh, "Increased photocatalytic activity of Zn(II)/Cu(II) oxides and sulfides by coupling and supporting them onto clinoptilolite nanoparticles in the degradation of benzophenone aqueous solution," *Journal of Hazardous Materials*, vol. 316, pp. 194–203, 2016.

[64] L. A. Pretzer, P. J. Carlson, and J. E. Boyd, "The effect of Pt oxidation state and concentration on the photocatalytic removal of aqueous ammonia with Pt-modified titania," *Journal of Photochemistry and Photobiology A: Chemistry*, vol. 200, no. 2-3, pp. 246–253, 2008.

[65] J. Lee, H. Park, and W. Choi, "Selective photocatalytic oxidation of NH_3 to N_2 on platinized TiO_2 in water," *Environmental Science and Technology*, vol. 36, no. 24, pp. 5462–5468, 2002.

[66] G. S. Pozan and A. Kambur, "Significant enhancement of photocatalytic activity over bifunctional ZnO–TiO_2 catalysts for 4-chlorophenol degradation," *Chemosphere*, vol. 105, pp. 152–159, 2014.

[67] R.-S. Juang, S.-H. Lin, and P.-Y. Hsueh, "Removal of binary azo dyes from water by UV-irradiated degradation in TiO_2 suspensions," *Journal of Hazardous Materials*, vol. 182, no. 1-3, pp. 820–826, 2010.

[68] M. A. Lazar, S. Varghese, and S. S. Nair, "Photocatalytic water treatment by titanium dioxide: recent updates," *Catalysts*, vol. 2, no. 4, pp. 572–601, 2012.